

Quantum confinement, core level shifts, and dopant segregation in P-doped Si⟨110⟩ nanowiresJiaxin Han,^{1,2} Tzu-Liang Chan,¹ and James R. Chelikowsky^{1,2,3}¹*Center for Computational Materials, Institute for Computational Engineering and Sciences, University of Texas at Austin, Austin, Texas 78712, USA*²*Department of Physics, University of Texas at Austin, Austin, Texas 78712, USA*³*Department of Chemical Engineering, University of Texas at Austin, Austin, Texas 78712, USA*

(Received 16 June 2010; revised manuscript received 14 September 2010; published 27 October 2010)

We examine P-doped Si⟨110⟩ nanowires by employing a real-space pseudopotential method. We find the defect wave function becomes more localized along the nanowire axis and the donor ionization energy increases, owing to quantum confinement. It is more difficult to dope a P atom into a Si⟨110⟩ nanowire than to dope Si bulk because the formation energy increases with decreasing size. By comparing the formation energy for different P positions within a nanowire, we find that if a P atom at the nanowire surface can overcome the energy barrier close to the surface, there is a tendency for the dopant to reside within the nanowire core. We calculate P core levels shift as P changes position within the nanowire and provide a means for x-ray photoelectron spectroscopy experiments to determine the location of P atoms within a Si nanowire.

DOI: [10.1103/PhysRevB.82.153413](https://doi.org/10.1103/PhysRevB.82.153413)

PACS number(s): 71.55.Cn, 73.21.Hb

Extensive semiconductor research has been focused on the nanoregimes over the past two decades. Within this regime, nanowires are one of the most technologically promising and widely studied nanostructures.¹ For example, logic gates have been assembled from nanowire building blocks, and used to implement basic computations² and fabricate field effect transistors.³ Nanowire-based biosensors have also been built and used for detecting a wide range of biological and chemical species.⁴ Given the existence of a well-developed Si-based microelectronic technology, Si nanowires are natural candidates for nanoscale electronic devices.

Previous theoretical studies on P-doped Si nanowires have focused on the effect of quantum confinement⁵ and the understanding of surface segregation of impurities.^{6–8} In particular, impurities segregated at the surface of a nanowire can dramatically reduce the density of carriers and have a detrimental effect on the transport property of a nanowire.⁹ As such, controlling the location of dopants within a nanowire for optimal device properties is of utmost importance. Here, we study the effect of quantum confinement on the defect wave function and the donor ionization energy of P-doped Si⟨110⟩ nanowires using first-principles calculations. We examine in detail the formation energy to dope a P atom into a Si⟨110⟩ nanowire as a function of nanowire diameter and position within the nanowire. We simulated the P core-level shift as P moves from the axis to the surface of a nanowire. We propose that core-level shift measurement by x-ray photoelectron spectroscopy (XPS) can be used to probe the position of P atoms inside Si nanowires.

Our calculations are based on pseudopotential-density functional theory¹⁰ using a real space grid code PARSEC.¹¹ The local spin-density approximation as determined by Ceperley-Alder¹² and parametrized by Perdew-Zunger¹³ is used for the exchange-correlation functional. The ionic pseudopotentials are constructed using the Troullier-Martins prescription¹⁴ in the Kleinman-Bylander form.¹⁵ The cubic grid spacing is 0.4 a.u. (1 a.u.=0.5292 Å), which is sufficient to converge the formation energies to within ~0.01 eV. Our structures are optimized so that the force on each atom is less than 0.001 Ryd/a.u. We focus on ⟨110⟩

nanowires as it is the preferred growth axis observed in experiments for wire diameter smaller than ~10 nm.¹⁶ The surface dangling bonds are passivated by H atoms. A passivated Si⟨110⟩ nanowire with a diameter of ~2 nm is illustrated in Figs. 1(a) and 1(b). Unless stated otherwise, our doped nanowires have one of the Si atoms close to the wire axis substituted by a P atom. A periodic boundary condition of periodicity 23.04 Å is imposed along the ⟨110⟩ axis direction. A cylindrical calculation domain encloses the Si⟨110⟩ nanowire and the wave function is set to zero at the domain boundary.¹⁷ We use 8 a.u. of vacuum space between the surface of the nanowire and the domain boundary, and consider only the Γ point for the Brillouin zone integration.

The electronic structure of a P-doped Si nanowire is characterized by a defect energy level in the energy gap as for the nanocrystal. In Fig. 1, we plot the charge density of the defect wave function of a P-doped Si⟨110⟩ nanowire. The charge density is elongated and localized along the wire axis. We integrate the charge density along the ⟨110⟩ axis direction (z direction) and the azimuthal angle ϕ . We illustrate the decay of the charge density along the radial coordinate r for three different P-doped Si⟨110⟩ nanowires in Fig. 1(c). The defect charge density has a maximum at $r=0$ where the P atom is located, and decays toward the nanowire surface. As the nanowire diameter decreases, the charge density becomes more localized at the center. As depicted in Fig. 1(c), the defect charge density can be fit very well to an exponential function of the form $K \exp(-2r/a_B)$, where K is a normalization constant and a_B is an effective Bohr radius that governs the decay of the charge density. We extract the effective Bohr radius, a_B , for P-doped Si⟨110⟩ nanowires with six different diameters. The result is plotted in Fig. 1(d). For the size range of the Si⟨110⟩ nanowires that we consider, the size dependence of a_B is roughly linear.

The donor ionization energy E_d (or activation energy) to promote an electron at the defect level to the conduction band minimum of a P-doped Si⟨110⟩ nanowire is of fundamental importance. E_d can be calculated by the difference between the Kohn-Sham eigenvalues of the defect level of a P-doped Si⟨110⟩ nanowire and the conduction band mini-

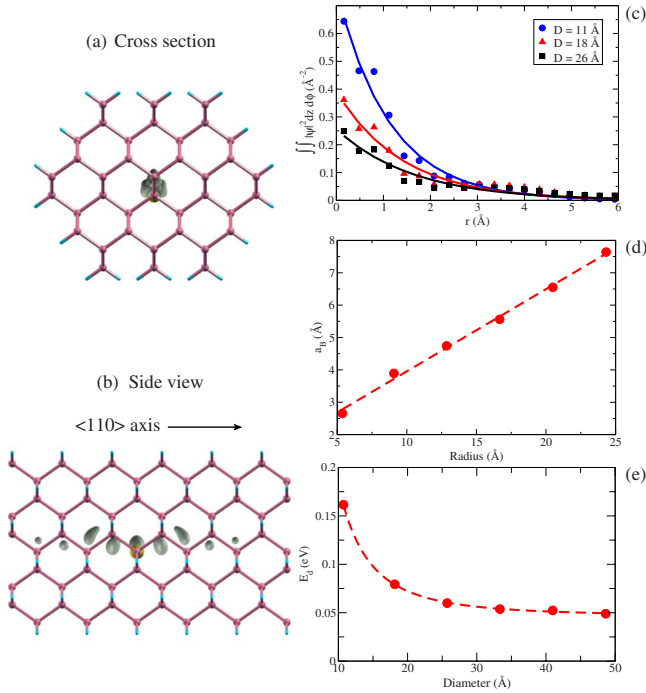


FIG. 1. (Color online) (a) The cross section and (b) side view of the defect charge density of a P-doped Si<110> nanowire. The large atom at the center is the P dopant. (c) The defect charge density plotted along the radial direction r with three different diameter D . The curves are fits using an exponential function of the form $K \exp(-2r/a_B)$. (d) Effective Bohr radius a_B plotted as a function of nanowire radius. The dashed line is a linear fit to our calculated data points: $1.4+R/3.9$. (e) Donor ionization energy E_d as a function of nanowire diameter. The dashed line is a fit to our calculated data points using a power law.

imum of a clean Si<110> nanowire of the same diameter. In Fig. 1(e), we plot E_d as a function of nanowire diameter. E_d increases with decreasing size owing to quantum confinement. A power law of the form $A+B/D^n$ can be fitted to our calculated values. Different values for the exponent n can provide clues on the physics that governs the trend of E_d . The fitting reveals that E_d has an asymptotic value $A=0.046$ eV as the diameter D goes to infinity, which is very close to the experimental bulk value of 0.044 eV. E_d remains close to the bulk limit till D decreases to ~ 3 nm, then it increases rapidly. n from our fit is 2.4. The exponent is quite close to 2, which suggests that the increase in E_d is dominated by the kinetic energy of a quantum well. Similar behavior of E_d is observed in other density-functional studies.^{18,19} Experimentally, E_d has a size dependence of $1/D$.^{20,21} The discrepancy between theoretical predictions and experimental observations implies that the ionized P atom is not immediately screened resulting in the P ion interacting with its induced charge on the nanowire surface.^{5,22} Such interaction gives rise to the $1/D$ dependence of the donor ionization energy for P-doped Si<110> nanowires and only happens after the system is ionized, therefore it is not captured by our Kohn-Sham eigenvalues calculated using a neutral system.

We study the formation energy of doping a Si<110> nanowire by P as a function of nanowire diameter and position

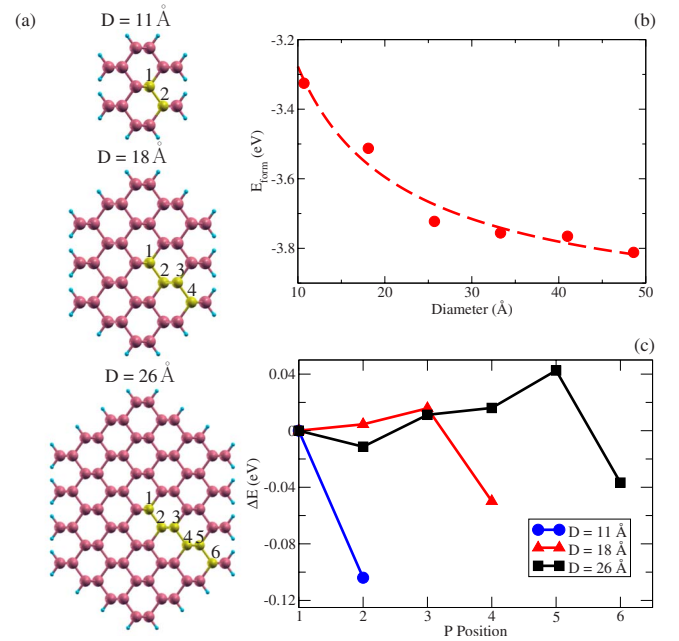


FIG. 2. (Color online) (a) Cross sections of three Si<110> nanowires with different diameter D . The number labels the different Si atoms that will be substituted by P. (b) The formation energy E_{form} as a function of nanowire diameter with the P at the nanowire axis. (c) Change in formation energy (ΔE) as P moves from the axis to the surface of a nanowire.

inside a nanowire. The formation energy is calculated by

$$E_{form} = E(\text{P-Si}) - E(\text{Si}) + \mu(\text{Si}) - \mu(\text{P}), \quad (1)$$

where $E(\text{P-Si})$ is the total energy of a P-doped Si<110> nanowire, and $E(\text{Si})$ is the total energy of a clean Si<110> nanowire of the same diameter. $\mu(\text{Si})$ is the chemical potential of Si. We assume that the replaced Si atom goes to a bulklike environment, and do not consider situations where the Si atom can stay at the surface of the nanowire, for example.²³ Here, we focus on the change in formation energy that originates from the effect of quantum confinement on the electronic structure. As such, $\mu(\text{Si})$ is simply taken to be the total energy of a Si atom in bulk. We use the total energy of an isolated P atom as the chemical potential $\mu(\text{P})$ for convenience. The value of $\mu(\text{P})$ depends on the experimental condition and the source of P used in experiments. Since we are only interested in the size dependence of E_{form} , the choice of $\mu(\text{P})$ can only shift E_{form} uniformly up or down and is not crucial for our purpose. Our calculated E_{form} is depicted in Fig. 2(b). E_{form} increases with decreasing diameter, i.e., it is increasingly more difficult to dope P atoms into a Si<110> nanowire as the wire diameter gets smaller. This behavior is similar to that in nanocrystals with magnetic dopants.²⁴ By extrapolation, we find that the formation energy at $D=1$ nm is ~ 0.7 eV higher than at the bulk limit.

In Fig. 2(c), we plot the change (ΔE) of E_{form} as a function of position within a Si<110> nanowire for three different diameters. E_{form} at position 1 is taken as the reference. We find that E_{form} has a bistable functional form in general: a basin that attracts a P atom toward the local minimum at the

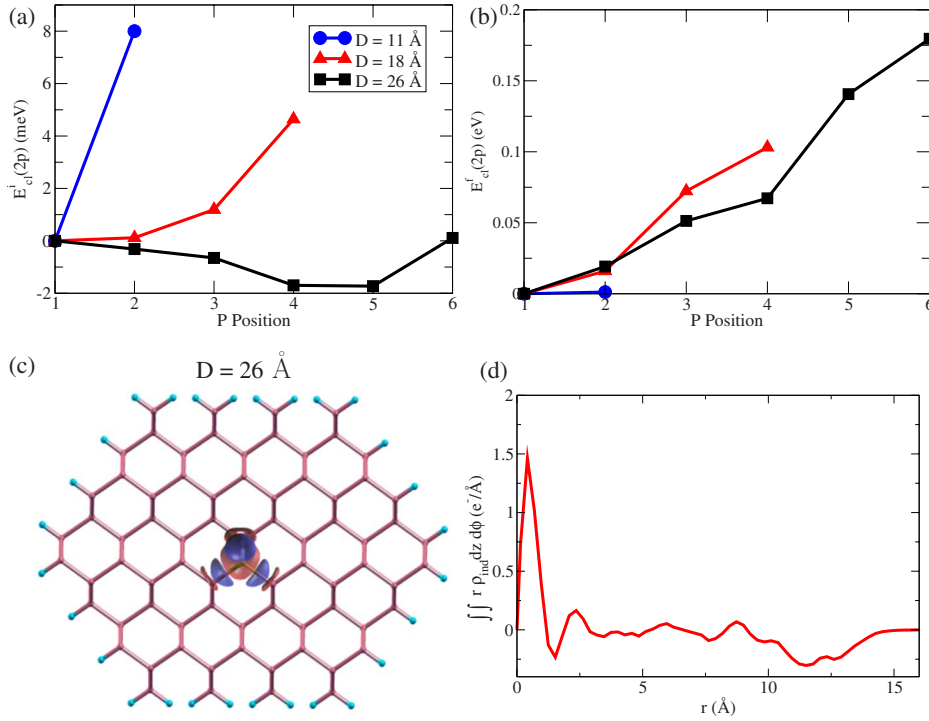


FIG. 3. (Color online) P $2p$ core level shift calculated using (a) initial-state theory and (b) final-state theory for P-doped Si(110) nanowires with three different diameter D . The P position for the x axis is labeled the same way as in Fig. 2(a). (c) A surface contour plot of the induced electronic charge ρ_{ind} owing to the ionized P atom at the axis of $D = 26$ Å Si nanowire. (d) The induced charge ρ_{ind} plotted as a function of the radial coordinate r . The origin is the location of the P atom.

axis of the nanowire, and a global minimum at the nanowire surface. As the diameter decreases, the spatial extent of the attractive basin shrinks. For the nanowire with the smallest diameter that we studied, the basin vanishes completely leaving behind the minimum at the surface. Without considering the position of P where a surface passivating H atom can form a bond directly with P, a similar qualitative trend can also be found in the literature.^{6,8} Our results suggest that if P atoms are introduced via the nanowire surface, there is an energy barrier that favors dopant surface segregation.

Core-level spectroscopy experiments using XPS can detect changes in the chemical environment of the P atom. As P position changes, the $2s$ and $2p$ core levels may change in response to the local chemical environment. By measuring the shift in the core levels, the experiment can infer whether the P atom is doped into the core of the Si nanowire or not. First, we simulate the $2s$ and $2p$ core-level shift as P position changes based on the initial state theory,²⁵ which is a first-order perturbation. The core-level shifts E_{cl}^i are the eigenvalues of a matrix G , whose matrix elements for a given angular momentum quantum number l and m are

$$G_{m_1, m_2}^l = \langle \phi_{l, m_1} | V_{scf} - V_{scf}^{ref} | \phi_{l, m_2} \rangle. \quad (2)$$

$\phi_{l, m}$ is either the $2s$ or $2p$ wave function of a P atom obtained by a separate all-electron calculation. $V_{scf}(V_{scf}^{ref})$ is the self-consistent potential of the (reference) system. To verify our scheme, we calculate the Si $2p$ core level shifts for $(\text{SiH}_3)_2\text{O}$ and SiClH_3 molecules using SiH_4 as the reference system. The shifts are found to be -0.61 eV and -1.1 eV, respectively, which are similar to -0.48 and -0.85 eV reported in Ref. 26 in terms of the sign, order of magnitude and the relative order. For a P-doped Si(110) nanowire, we choose the Si nanowire with the P atom at the center of the wire as the reference system. V_{scf} and V_{scf}^{ref} are aligned such that the P

atom in both systems have the same coordinate. In other words, we calculate the perturbation of the self-consistent potential at the P atom when the P moves away from the wire axis toward the surface. The perturbation leads to a shift in the $2s$ and $2p$ core levels of P. In Fig. 3(a), we plot the $2p$ core-level shift $E_{cl}^i(2p)$ as P moves from the center toward the nanowire surface for three different nanowires. We find that the self-consistent potential at the P core is nearly isotropic. Only the average of the three eigenvalues for the $2p$ state is plotted as they are nearly degenerate. The plot for the $2s$ core level shift $E_{cl}^i(2s)$ is qualitatively the same. The core-level shift predicted by the initial-state theory is very small (<0.01 eV). This is because there are no changes in the chemical environment as P moves within the Si nanowire as we limit the P from bonding with the surface H.

Alternatively, the core-level shift can be predicted by the final-state theory, where the relaxation of the valence electron owing to the removal of a core electron can be taken into account. For the final-state theory, we directly calculate the ionization energy of the $2s$ and $2p$ core electrons of P. The core-level shift corresponds to the change in core-level ionization energy as P moves from the center toward the nanowire surface

$$E_{cl}^f = (E_i - E_0) - (E_i^{ref} - E_0^{ref}). \quad (3)$$

E_0 and E_i are the total energies of a P-doped Si(110) nanowire before and after the ionization of a core electron, respectively. E_0^{ref} and E_i^{ref} are the corresponding total energies for the reference system. The calculation of E_i and E_i^{ref} can be done by generating a new pseudopotential for P with either $2s$ or $2p$ electron removed. The pseudopotential corresponds to an ionized configuration. Consequently, E_i and E_i^{ref} involves calculating charged nanowires. We fill the cylindrical calculation domain enclosing the charged nanowire by a

compensating jellium such that the system is neutral. We checked that our results are insensitive to the diameter of the calculation domain. Although the interaction between charges in different periodic images is long range, the error in E_i and E_i^{ref} should be very similar and cancel in the calculation of core-level shift. Note that the atomic geometry for the evaluation of E_i is kept to be the same as E_0 because XPS event (10^{-16} s) is much shorter than the vibration time scale (10^{-13} s). We also calculate the Si $2p$ core level shifts for $(\text{SiH}_3)_2\text{O}$ and SiClH_3 molecules using the final-state theory as a check. Our results are -1.00 eV and -1.18 eV, respectively, which agree well with -0.94 and -0.99 eV obtained in Ref. 26.

Our calculated results for $E_{cl}^f(2p)$ for three different Si nanowires are plotted in Fig. 3(b). $E_{cl}^f(2s)$ is not shown because it is nearly the same as $E_{cl}^f(2p)$. By comparing $E_{cl}^f(2p)$ and $E_{cl}^i(2p)$, we find that the core-level shift is mainly contributed by the final-state effect, which is on the order of 0.1 eV except for the smallest nanowire. High-resolution XPS can probe the first few atomic layers below the surface and should have an energy resolution ~ 0.1 eV, see for example Ref. 27. Therefore, we expect the diffusion of P into a Si nanowire through the surface can be measured by core-level shift experiments. $E_{cl}^f(2p)$ is positive means that the ionization energy of the $2p$ core electron is higher as P approaches the nanowire surface. Our initial-state results suggest that the changes in the core-level eigenvalue is small within the nanowire. The higher ionization energies obtained by the final-state theory imply that the total energy E_i with P ionized increases toward the surface. In order to understand the origin of the energy increase, we study the induced electronic charge ρ_{ind} after the core $2p$ electron is stripped away from the P atom. ρ_{ind} is obtained by the difference between the total electronic charge density before and after the ionization. Figure 3(c) illustrates ρ_{ind} when the P is located at the nano-

wire axis. We also plot the radial distribution of ρ_{ind} (the location of P is taken as the origin) in Fig. 3(d) by integrating the azimuthal ϕ and axial z coordinates. Without the $2p$ electron, the P atom becomes positively charged and draws electrons close to it from the nanowire surface. This is indicated by the positive (electron excess) ρ_{ind} close to the origin which becomes negative (electron deficit) at the surface in Fig. 3(d). As P moves toward the nanowire surface, we find that the amount of induced electronic charge close to the P atom changes very little. Therefore, the increase in E_i toward the surface is not related to changes in screening unless the P is nearly at the surface. Instead, the behavior of E_i can be understood by a decrease in the polarization energy stored in the Si dielectric nanowire as an embedded charge moves toward the surface.

In summary, we present a first-principles study of P-doped Si<110> nanowires. Owing to quantum confinement, the defect wave function becomes more localized along the wire axis, and the donor ionization energy increases with decreasing wire diameter. In addition, the formation energy to dope a P atom into a Si<110> nanowire increases with decreasing size. By examining the formation energy as a function of P position within a nanowire, we find that there are two stable positions for P: one at the wire axis and the other at the surface. We simulate the P $2s$ and $2p$ core-level shifts for different P positions inside a Si<110> nanowire using both initial-state and final-state method. We find that the core-level shift mainly comes from the final-state effect, and the core-level ionization energy is higher when the P atom moves toward the surface.

We would like to acknowledge support by the U.S. Department of Energy, Office of Basic Energy Sciences and Office of Advanced Scientific Computing Research (Grants No. DE-FG02-06ER15760 on nanostructures and No. DE-SC000187 on algorithms, respectively). Computational resources were provided in part by NERSC and TACC.

-
- ¹R. Rurali, *Rev. Mod. Phys.* **82**, 427 (2010).
²Y. Huang *et al.*, *Science* **294**, 1313 (2001).
³G. Zheng, W. Lu, S. Jin, and C. M. Lieber, *Adv. Mater.* **16**, 1890 (2004).
⁴F. Patolsky, G. Zheng, and C. M. Lieber, *Anal. Chem.* **78**, 4260 (2006).
⁵M. Diarra, Y.-M. Niquet, C. Delerue, and G. Allan, *Phys. Rev. B* **75**, 045301 (2007).
⁶H. Peelaers, B. Partoens, and F. M. Peeters, *Nano Lett.* **6**, 2781 (2006).
⁷E. Durgun, N. Akman, C. Ataca, and S. Ciraci, *Phys. Rev. B* **76**, 245323 (2007).
⁸C. R. Leao, A. Fazzio, and A. J. R. da Silva, *Nano Lett.* **8**, 1866 (2008).
⁹M. V. Fernández-Serra, Ch. Adessi, and X. Blase, *Phys. Rev. Lett.* **96**, 166805 (2006).
¹⁰W. Kohn and L. J. Sham, *Phys. Rev.* **140**, A1133 (1965).
¹¹J. R. Chelikowsky, N. Troullier, and Y. Saad, *Phys. Rev. Lett.* **72**, 1240 (1994).
¹²D. M. Ceperley and B. J. Alder, *Phys. Rev. Lett.* **45**, 566 (1980).
¹³J. P. Perdew and Y. Wang, *Phys. Rev. B* **45**, 13244 (1992).
¹⁴N. Troullier and J. L. Martins, *Phys. Rev. B* **43**, 1993 (1991).
¹⁵L. Kleinman and D. M. Bylander, *Phys. Rev. Lett.* **48**, 1425 (1982).
¹⁶Y. Wu, Y. Cui, L. Huynh, C. Barrelet, D. Bell, and C. Lieber, *Nano Lett.* **4**, 433 (2004).
¹⁷J. Han, M. L. Tiago, T.-L. Chan, and J. R. Chelikowsky, *J. Chem. Phys.* **129**, 144109 (2008).
¹⁸R. Rurali, B. Aradi, T. Frauenheim, and A. Gali, *Phys. Rev. B* **79**, 115303 (2009).
¹⁹F. Bruneval, *Phys. Rev. Lett.* **103**, 176403 (2009).
²⁰M. T. Björk, H. Schmid, J. Knoch, H. Riel, and W. Riess, *Nat. Nanotechnol.* **4**, 103 (2009).
²¹J. Yoon *et al.*, *Appl. Phys. Lett.* **94**, 142102 (2009).
²²Y. M. Niquet, L. Genovese, C. Delerue, and T. Deutsch, *Phys. Rev. B* **81**, 161301 (2010).
²³R. Rurali and X. Cartoixà, *Nano Lett.* **9**, 975 (2009).
²⁴G. M. Dalpian and J. R. Chelikowsky, *Phys. Rev. Lett.* **96**, 226802 (2006).
²⁵X. Blase, A. J. R. da Silva, X. Zhu, and S. G. Louie, *Phys. Rev. B* **50**, 8102 (1994).
²⁶A. Pasquarello, M. S. Hybertsen, and R. Car, *Phys. Rev. B* **53**, 10942 (1996).
²⁷A. Santoni *et al.*, *J. Phys.: Condens. Matter* **18**, 10853 (2006).